CONSTRAINTS ON THE PROTON PARTON DISTRIBUTION FUNCTIONS FROM THE LARGE HADRON COLLIDER

M.R. Sutton
Department of Physics and Astronomy, The University of Sussex, Falmer, Brighton BN1 9QH, United Kingdom

On behalf of the
ATLAS and CMS Collaborations

Recent results on cross sections sensitive to the parton distribution functions (PDFs) within the proton from the ATLAS and CMS Collaborations are presented. The potential impact on the inclusion of this data in fits to the PDFs is discussed and a recent fit including the data on vector boson production from the ATLAS experiment is discussed.

1 Introduction

The LHC is an exemplary machine for the study of perturbative QCD. All processes at the LHC take place between quarks and gluons so given sufficient understanding of the hard sub-process any process could in principle be used to constrain the parton density functions (PDFs) within the proton – an essential prerequisite if we are to identify and understand any possible signature of physics beyond the Standard Model.

Since the first collisions at the end of 2009, the LHC has performed well beyond expectation, with integrated luminosities collected by both the ATLAS [1] and CMS [2] experiments of around 5 fb^{-1} collected with beam energies of 7 TeV. Even at this lower than design beam energy, the kinematic region accessible at the LHC is orders of magnitude larger in Q^2 than available at either HERA or the Tevatron, and extends the available range of the proton momentum fraction, x, to values many orders of magnitude smaller than accessible at the Tevatron. Although these values were accessible at HERA, this was at correspondingly low values of Q^2, at or below a few GeV^2. At the LHC, this low-x region will be accessible for $Q^2 > 100$ GeV^2, so for the first time, it will be possible to study low-x physics at truly perturbative scales.

As a consequence of this larger kinematic plane, cross sections at high transverse energy, E_T, which were dominated by quark-antiquark scattering at the Tevatron, have a larger, or even dominant contribution from processes containing gluons in the initial state. This means that processes for example involving jets at high E_T will allow better constraints on the gluon distribution at higher x and measurement of the strong coupling α_S at significantly higher scales than previously. In addition, the copious production of electroweak bosons – $W^{\pm}$ and Z^0 – at high energies should allow more stringent constraints on the quark distributions at intermediate and high-x due to the direct coupling of the quarks to the vector bosons and relatively small backgrounds from pure QCD events.

1.1 Global Fits

The QCD splitting functions have been available at Next-to-Next-to-Leading order (NNLO) for some time [3] together with the coefficient functions for vector boson production [4,5] and Deep Inelastic Scattering (DIS) [6]. At present the full matrix elements for the full calculation of the QCD Jet cross section is not available. As such, fits including the DIS data from HERA and fixed target experiments and vector boson production data at NNLO are available. These fits may include jet data from HERA, the Tevatron or the LHC, but only at Next-to-Leading order (NLO). Numerous fits for the proton PDFs are available[7–13], each considering slightly different data samples and with different parametrisations or treatment of Heavy Flavour, such that

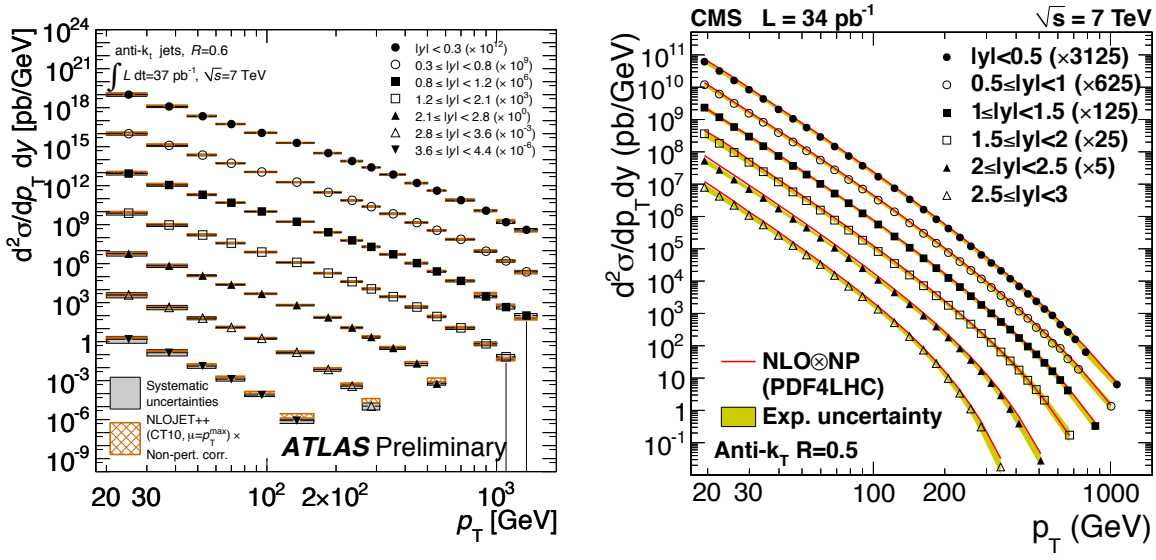

Figure 1: The inclusive single jet cross section from the ATLAS and CMS Collaborations, doubly differential in jet P_T and rapidity.

significant differences still exist between parametrisations at LHC energies [14] so the inclusion of LHC data has the potential to provide significantly better constraints.

2 LHC Data

2.1 Inclusive jet data

The inclusive single jet cross sections from the ATLAS and CMS Collaborations [15,16] are shown in Figure 1. The predictions of NLO QCD agree well with the measured cross sections over more than 8 orders of magnitude for both the ATLAS and CMS cross sections over the entire range of the jet rapidity.

Except at the highest jet P_T, where the statistical uncertainties are large, the data are limited by the systematic uncertainty. In both cases, the largest uncertainty is that arising from uncertainties in the Jet Energy Scale which typically ranges from around 1% to 7% for calorimeter based jets and at high P_T is predominantly due to the modeling of the single particle response in the calorimeter [17] and is illustrated in Figure 2. This typically leads to large uncertainties, $\mathcal{O}(10-20\%)$ on the steeply falling jet cross section.

Using a particle flow algorithm, where individual calorimeter clusters are matched to tracks before jet finding, to take account of the better energy resolution of low P_T tracks, the CMS Collaboration are able to obtain a Jet Energy Scale systematic uncertainty of around 2% for jets with P_T 100 GeV [18], also illustrated in Figure 2. This type of analysis will be essential, together with a full understanding of the complete correlation of the various components of the systematic uncertainty in order to obtain the optimal constraint from the Jet cross section.

Figure 3 shows the inclusive dijet cross section from the ATLAS and CMS Collaborations [15,19] versus the dijet invariant mass, differentially in the rapidity of the dijet system illustrating that the data are well described by the NLO calculation again over an 8 orders of magnitude variation of the cross section.

As in the case of the inclusive single jet cross section, the largest uncertainty is that arising from the Jet Energy Scale. In this case, however, the selection on the sub-leading jet allows a better control over the kinematics of the incoming partons and greater sensitivity to their momentum fraction x although at the cost of larger renormalisation scale uncertainties on the

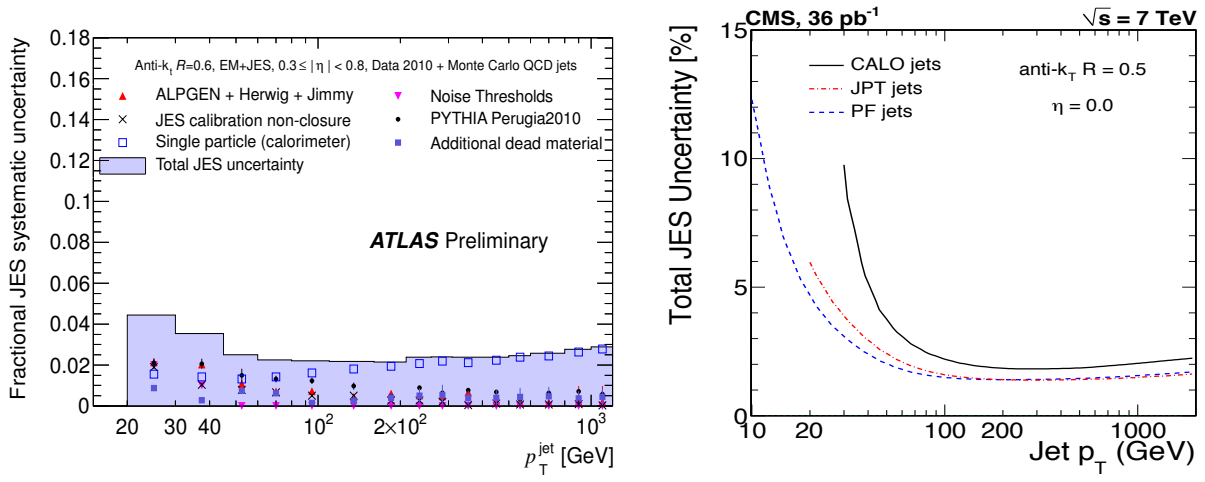

Figure 2: The Jet Energy Scale (JES) Uncertainty for central jet production from the ATLAS and CMS collaborations. The CMS uncertainties are those for calorimeter based (CALO) jets, calorimeter jets with track information (JPT) and Particle Flow (PF) jets. The ATLAS plot shows the different contributions to the overall JES uncertainty.

calculation.

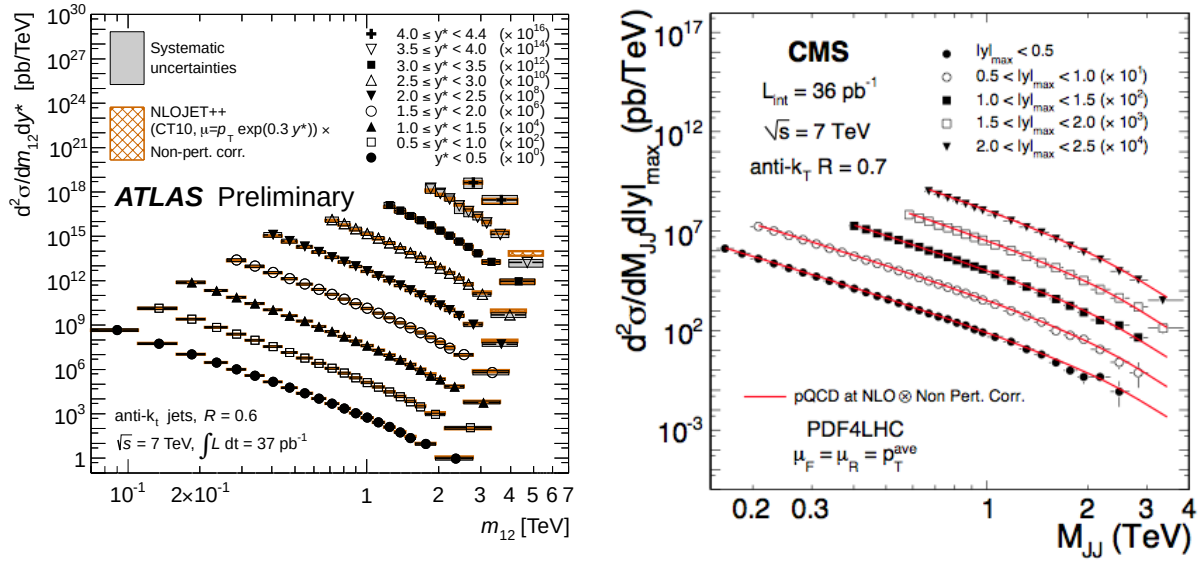

Figure 3: The inclusive dijet cross section from the ATLAS and CMS Collaborations, doubly differential in the dijet invariant mass and the dijet rapidity.

2.2 Vector boson production

At the LHC, W and Z bosons are produced copiously with $\mathcal{O}(10^7)$ $W^{\pm}$ and $\mathcal{O}(10^6)$ Z bosons expected per fb^{-1}. The Drell-Yan cross section is known to NNLO with a theoretical uncertainty of around 5% [4,5]. As such the lepton distributions from vector boson production should be well described and the ability to reconstruct electrons or muons means that the measurement will be insensitive to the jet energy scale.

The large available sample of the vector boson data, particularly the data on the W charge asymmetry, means that the experimental uncertainties on the cross sections are smaller than the differences between the available parton distributions. Figure 4 shows the total cross section

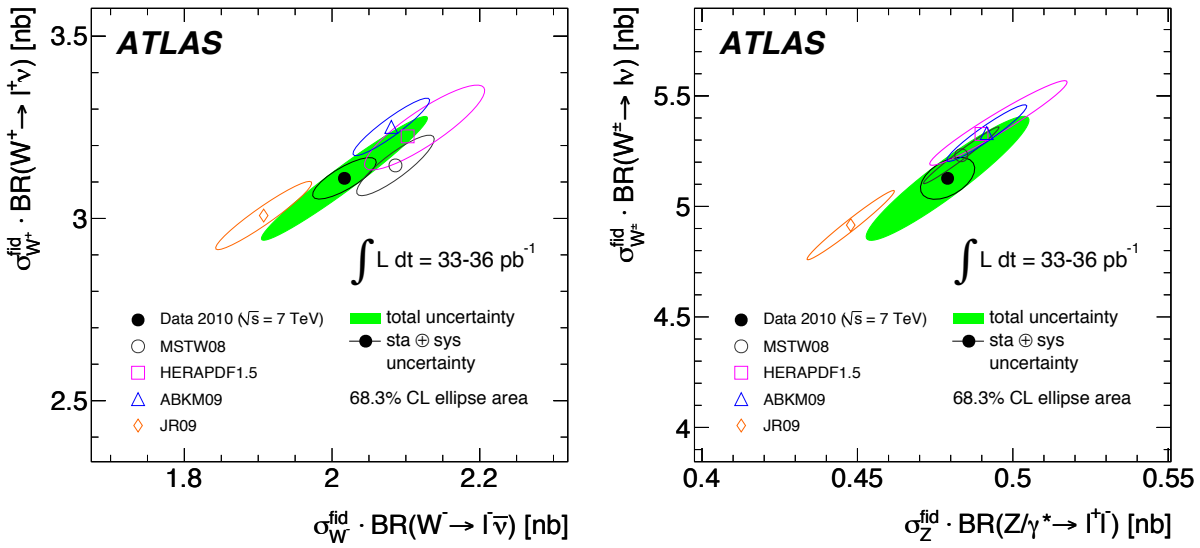

Figure 4: The cross section times branching ratio for W and Z production with respect to each other from the ATLAS collaboration.

times branching ratio for W^+ production versus W^- production, and for combined $W^\pm$ production versus the Z cross section times branching ratio from the ATLAS Collaboration [20]. The data are for the observable cross section in the measureable fiducial region and are not corrected to the full phase space of the vector boson. Also shown are the predictions from several NLO parton distributions showing that these data have the potential to discriminate between the different available fits. None of the PDFs shown include these data in the fit.

The large data sample available, means that besides the total observable cross sections, the measurement of distributions more differential in the kinematic variables is also possible. Assuming the equality of the u and d sea quark densities and neglecting the heavy flavour contribution, the W charge asymmetry should be sensitive to the difference between the u_v and d_v valence quark densities,

$$A_W \approx \frac{u_v - d_v}{u + d}, \tag{1}$$

where u and d are the full quark densities. Since the neutrino from the W decay would not be observed, this would require extrapolation for the W decay. Avoiding this extrapolation, Figure 5 shows the lepton charge asymmetry for $W^\pm$ production from ATLAS [20] and CMS [21], defined by

$$A_l = \frac{d\sigma(W^+ \to l^+\nu)/d\eta_{l^+} - d\sigma(W^- \to l^-\bar{\nu})/d\eta_{l^-}}{d\sigma(W^+ \to l^+\nu)/d\eta_{l^+} + d\sigma(W^- \to l^-\bar{\nu})/d\eta_{l^-}}, \tag{2}$$

which makes use of the correlation of the lepton direction with the W boson direction so that that there is good correlation of this variable with the W charge asymmetry without the need to correct the W kinematics for the unobserved neutrino energy. Also shown in Figure 5 are the LHCb [22] cross section [23] and predictions from the CTEQ6.6 [24], CTEQ10 [7], HERAPDF [10,11], MSTW [8], ABKM [12] and JR [13] fits. The CTEQ and HERAPDF predictions lie at the upper limit of the data at small rapidities whereas the MSTW prediction lies slightly below the data in this region and the HERAPDF lies below the data at larger rapidities.

At very large rapidities – beyond the ATLAS and CMS acceptance – the LHCb measurement, which extends the measurement by more than two units of pseudo-rapidity, seems to favour slightly the JR prediction although the theoretical uncertainties are large. The inclusion of these data in the fits should have the potential to significantly improve the uncertainties on the quark distributions at intermediate x.

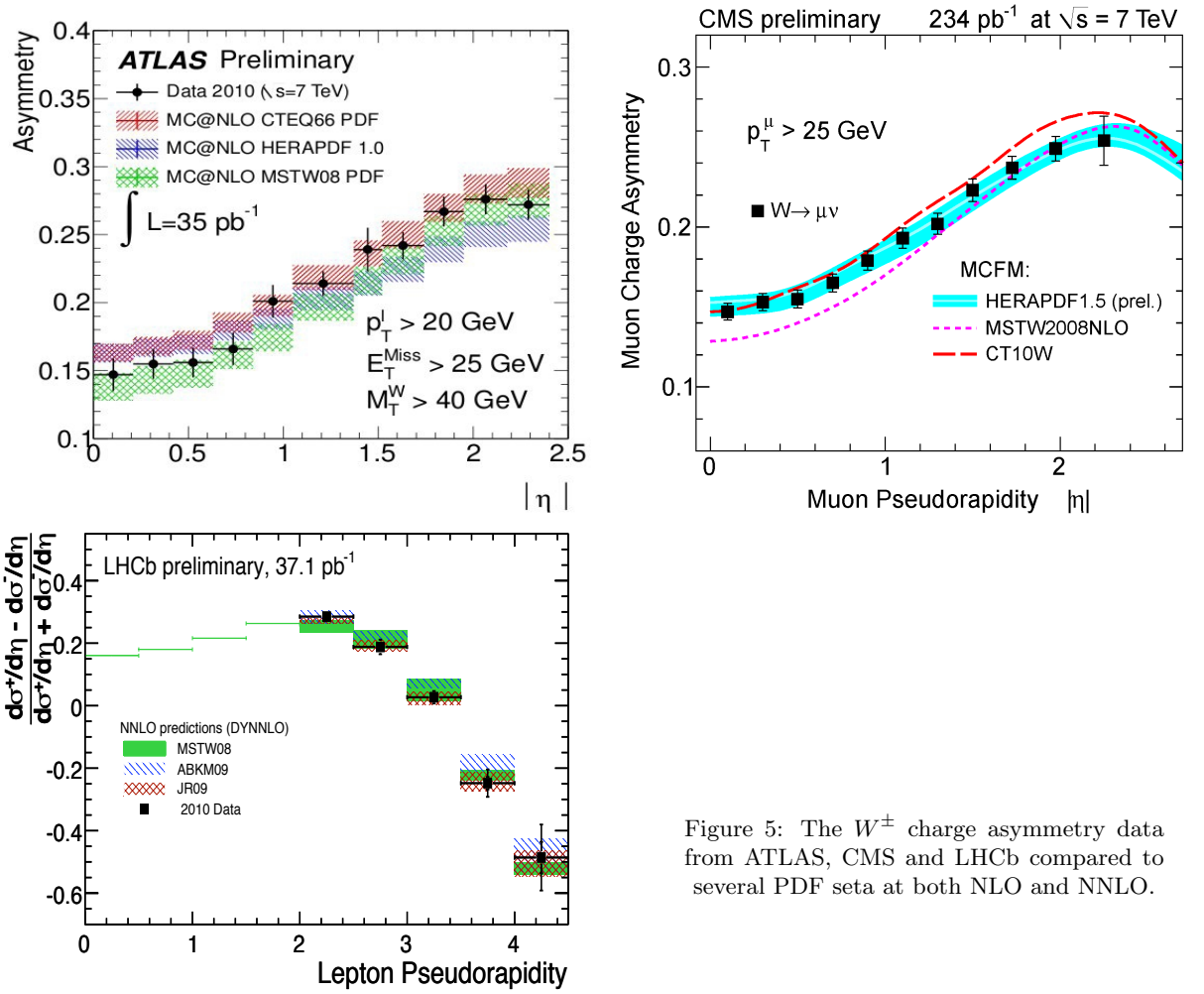

Figure 5: The $W^{\pm}$ charge asymmetry data from ATLAS, CMS and LHCb compared to several PDF seta at both NLO and NNLO.

The inclusive vector boson production will provide better constraints for scales around the mass of the respective bosons. The large data sample also means that data on the production of vector bosons with associated high E_T jets will also allow harder scales to be probed. In this case however, the calculations may suffer from large logarithms which would need to be resummed. In addition, with sufficient statistics, the measurement of W bosons in events with associated tagged, charmed or bottom quark initiated jets should allow better discrimination of the initial quark flavour and provide further sensitive constraints.

3 Fits including the LHC data

The first fits to include LHC data are becoming available [25,26]. At present, the large systematic uncertainties on the jet data mean that the predictions from all PDFs are currently in agreement with the data and only a small improvement in the gluon uncertainty is currently observed, although the analysis of the full available data set and understanding of the full correlated uncertainties should still provide a reasonable constraint, becoming significantly better as the Jet Energy Scale is improved.

Fits from the NNPDF group suggest that the uncertainty on the u and d densities are somewhat smaller [25] when including 36 pb^{-1} of W and Z data, so it will be interesting to see the impact on the fits from the newer LHC data. Recently, new QCD fits including the most recent data on the W^+, W^- and Z boson rapidity distributions have been performed by the

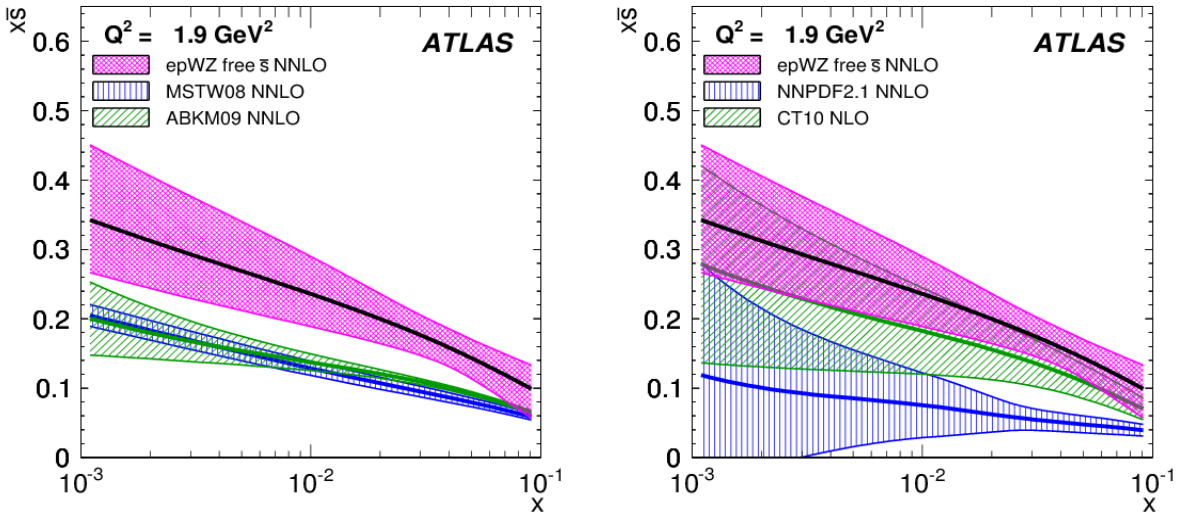

Figure 6: The $\bar{s}$ quark density from the recent ATLAS NNLO fit compared to several global fits at NLO and NNLO.

ATLAS Collaboration [26]. Fits where the s and $\bar{s}$ densities are constrained to be the same, and are allowed to vary independently have been performed at NNLO using the NLO predictions from MCFM [27] and NNLO K factors from from FEWZ [28] and DYNNLO [29].

Figure 6 shows the $\bar{s}$ quark density from the ATLAS fit where the $\bar{s}$ quark density is allowed to vary independently in contrast to the usual constraint that $\bar{s}/\bar{d} = 0.5$ [8,9,12]. This fit suggests that the $\bar{s}/s$ ratio is $1.00^{+0.025}_{-0.028}$ at $x = 0.023$ but, as seen in the Figure, the $\bar{s}$ quark density is larger than that obtained from the global fits from elsewhere. Although this reduces the $\bar{u}$ and $\bar{d}$ sea quark distributions, which are correlated through the overall normalisation, the precise DIS data and sum rules, the overall result is a combined sea quark density around 8% larger than the global fits.

4 Conclusions

A large portfolio of high precision data are available from the LHC experiments. Significantly larger data sets are already available and a great deal of work is underway to better understand the systematic uncertainties so that higher precision data with smaller statistical uncertainties at large scales will be available soon.

At present the inclusion of this new data in global fits is understandably rather limited, but new fits from the PDF fitting community should be available soon and should provide us with a significantly better understanding of the proton PDF at unprecedentedly large scales.

5 Acknowledgements

The author would like to thank the University of Sussex for funding to attend the workshop and the workshop Organising Committee for a most interesting workshop.

References

1. ATLAS Collaboration; JINST 3:S08003 (2008).
2. CMS Collaboration; JINST 3:S08004 (2008).
3. S. Moch *at al*; *Nucl. Phys.* B**688**, 101 (2004); *Nucl. Phys.* B**691**, 129 (2004).

4. R. Hamberg *et al*; *Nucl. Phys.* B**359**, 343 (1991); [Erratum ibid. B**644**, 403 (2002)].
5. R.V. Harlander and W.B. Kilgore; *Phys. Rev. Lett.* **88**, 201801 (2002).
6. S. Moch *at al*; *Phys. Lett.* B**606**, 123 (2005); hep-ph/0504242 (2005).
7. H.-L. Lai *et al*; *Phys. Rev.* D**82**, 074024 (2010).
8. A. Martin *et al*; *Eur. Phys. J.* **C63**, 189 (2009).
9. R. D. Ball *et al*; *Nucl. Phys.* B**809**, 1 (2009); *Nucl. Phys.* B**855**, 153 (2012).
10. F. D. Aaron *et al* (H1 and ZEUS Collaborations), JHEP**01**, 109 (2010).
11. V. Radescu; (2011), H1prelim-11-042, ZEUS-prel-11-002, Proceedings of Moriond 2011, arXiv:1107.4193 [hep-ex] (2011).
12. S. Alekhin *et al*; *Phys. Rev.* D**81**, 014032 (2010).
13. P. Jimenez-Delgado and E. Reya; *Phys. Rev.* D**79**, 074023 (2009); arXiv:0810.4274 [hep-ph] (2008).
14. G. Watt; arXiv:1106.5788v2 [hep-ph] (2011); JHEP**09**, 069 (2011).
15. ATLAS Collaboration; arXiv:1112.6297v1 [hep-ex] (2011).
16. CMS Collaboration; *Phys. Rev. Lett.* **107** 132001 (2011).
17. ATLAS Collaboration; ATLAS-CONF-2011-032 (2011).
18. CMS Collaboration; *J. Instrum.* 6 P11002 (2011).
19. CMS Collaboration; *Phys. Lett.* B**700** 187 (2011).
20. ATLAS Collaboration; arXiv:1109.5141 [hep-ex] (2011) to be published in *Phys. Rev.* D.
21. CMS Collaboration; CMS-PAS-EWK-11-005 (2011).
22. LHCb Collaboration; JINST 3:S08005 (2008).
23. LHCb Collaboration; LHCb-CONF-2011-039 (2011); arXiv:1204.1620v1 [hep-ex] (2012).
24. P. M. Nadolsky *et al*; *Phys. Rev.* D**78**, 013004 (2008); arXiv:0802.0007 [hep-ph] (2008).
25. J. Rojo; "NNPDF Update" presentation at the PDF4LHC Forum, Dec. 2011, `https://indico.cern.ch/conferenceOtherViews.py?confId=145744`.
26. The ALTAS Collaboration; arXiv:1203.4051v1 [hep-ex] (2012) submitted to *Phys. Rev. Lett.*.
27. J. M. Campbell and R. K. Ellis; *Nucl. Phys. Proc. Suppl.* **205-206**, 10 (2010).
28. R. Gavin *et al*; *Comput. Phys. Commun.* **182** 2388-2403 (2011).
29. S. Catani *et al*; *Phys. Rev. Lett.* **103**, 082001 (2009).